molecular pharmaceutics

Article

pubs.acs.org/molecularpharmaceutics

Liposomal Delivery of Diacylglycerol Lipase-Beta Inhibitors to Macrophages Dramatically Enhances Selectivity and Efficacy *in Vivo*

Myungsun Shin,[†,#] Helena W. Snyder,[∥,#] Giulia Donvito,[⊥] Lesley D. Schurman,[⊥] Todd E. Fox,[‡,§] Aron H. Lichtman,[⊥] Mark Kester,[‡,§] and Ku-Lung Hsu*[,†,‡]

[†]Department of Chemistry, University of Virginia, Charlottesville, Virginia 22904, United States
[‡]Department of Pharmacology, University of Virginia, Charlottesville, Virginia 22908, United States
[§]University of Virginia Cancer Center, University of Virginia, Charlottesville, Virginia 22903, United States
[∥]Department of Materials Science and Engineering, University of Virginia, Charlottesville, Virginia 22904, United States
[⊥]Department of Pharmacology and Toxicology, Virginia Commonwealth University, Richmond, Virginia 23298 United States

Supporting Information

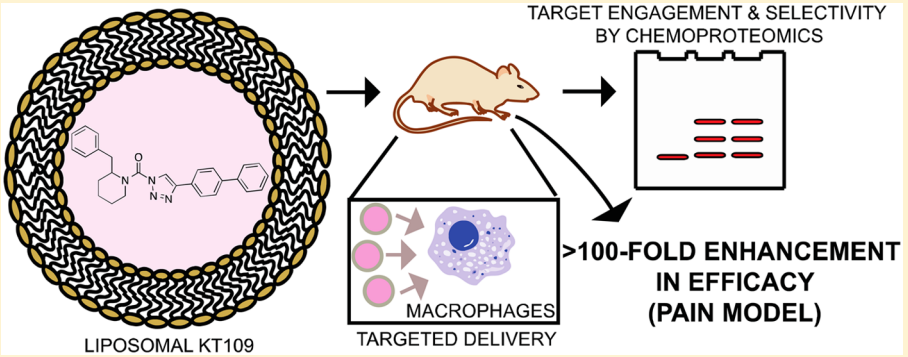

ABSTRACT: Diacylglycerol lipase-beta (DAGLβ) hydrolyzes arachidonic acid (AA)-containing diacylglycerols to produce bioactive lipids including endocannabinoids and AA-derived eicosanoids involved in regulation of inflammatory signaling. Previously, we demonstrated that DAGLβ inactivation using the triazole urea inhibitor KT109 blocked macrophage inflammatory signaling and reversed allodynic responses of mice in inflammatory and neuropathic pain models. Here, we tested whether we could exploit the phagocytic capacity of macrophages to localize delivery of DAGLβ inhibitors to these cells *in vivo* using liposome encapsulated KT109. We used DAGLβ-tailored activity-based probes and chemical proteomic methods to measure potency and selectivity of liposomal KT109 in macrophages and tissues from treated mice. Surprisingly, delivery of ~5 μg of liposomal KT109 was sufficient to achieve ~80% inactivation of DAGLβ in macrophages with no apparent activity in other tissues *in vivo*. Our macrophage-targeted delivery resulted in a >100-fold enhancement in antinociceptive potency compared with free compound in a mouse inflammatory pain model. Our studies describe a novel anti-inflammatory strategy that is achieved by targeted *in vivo* delivery of DAGLβ inhibitors to macrophages.

KEYWORDS: *endocannabinoid, 2-arachidonoylglycerol, diacylglycerol lipase, macrophage, inflammation, activity based protein profiling, chemical proteomics, diacylglycerol, prostaglandin, eicosanoid, lipid signaling, chronic pain, neuropathic pain, inflammation, nonsteroidal anti-inflammatory drugs, analgesic, liposome, drug delivery, pain*

INTRODUCTION

Diacylglycerol lipases[1−4] (DAGLs) are principal biosynthetic enzymes for the endocannabinoid 2-arachidonoylglycerol (2-AG[5,6]), a lipid agonist of the GPCRs CB1 and CB2.[7] DAGLs are transmembrane serine hydrolases that hydrolyze arachidonate-esterified diacylglycerols (DAGs) to biosynthesize 2-AG, which can be further cleaved by downstream enzymes to release arachidonic acid (AA) for cyclooxygenase (COX)-mediated eicosanoid production (e.g., PGE2, Figure 1). The regulation of both 2-AG and AA by DAGLs not only establishes important cross-talk between endocannabinoid and eicosanoid signaling[4,8] but also offers new opportunities for blocking inflammation using DAGL-selective inhibitors.[4,9−15] Two mammalian isoforms, DAGLα and DAGLβ, have been identified, and development of chemical proteomic[4,15] and genetic tools[2,3] have enabled investigation of isoform-specific functions that are separated anatomically and even by cell type

Special Issue: Pharmacology by Chemical Biology

Received: July 31, 2017
Revised: August 21, 2017
Accepted: August 30, 2017

DOI: 10.1021/acs.molpharmaceut.7b00657
Mol. Pharmaceutics XXXX, XXX, XXX−XXX

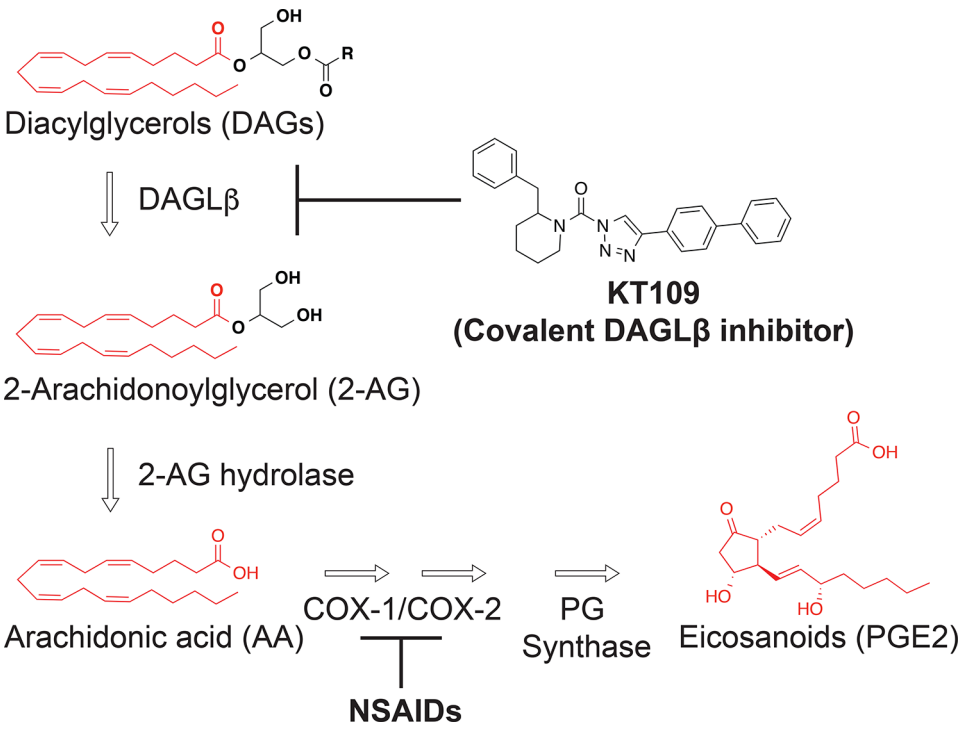

Figure 1. DAGLβ hydrolyzes DAGs to regulate lipid precursors important for inflammation. DAGLβ hydrolyzes diacylglycerol (DAG) to produce 2-arachidonoylglycerol (2-AG). DAG can signal by activating protein kinase pathways and 2-AG is the predominant lipid messenger for cannabinoid receptors. 2-AG can be further hydrolyzed by a downstream serine hydrolase (2-AG hydrolase) to produce arachidonic acid (AA), which is a substrate for cyclooxygenase 1 and 2 enzymes (COX1/2). COX1/2 along with PG synthases biosynthesize eicosanoids including PGE2, which signal through prostaglandin receptors. Nonsteroidal anti-inflammatory drugs (NSAIDs) block COX1/2 activity.

within the same tissue.[9] From these studies, DAGLβ has emerged as the isoform with a more specialized role in inflammation because of its enriched expression and activity in macrophages[4] and microglia,[9] and its role in regulating proinflammatory lipid (PGE2) and cytokine (TNF-α) pathways.[4]

Discovery of first generation DAGLβ inhibitors was enabled by development of tailored activity-based protein profiling (ABPP) methods to overcome challenges with detection and quantitation of native DAGL activity.[4,15] In addition to being highly sensitive, ABPP methods allowed rapid evaluation of DAGLβ inhibitor potency and selectivity directly in complex lysates. Using chemical proteomics to guide inhibitor optimization, the 1,2,3-triazole urea inhibitor KT109 emerged as the first *in vivo*-active DAGLβ inhibitor suitable for cell and animal physiology studies.[4,11] Subsequent studies have since adopted this strategy to expand development of covalent as well as reversible DAGL inhibitors.[10,13,14,16] Cell biology studies using DAGLβ inhibitors showed potent reductions in PGE2 as well as TNF-α signaling in lipopolysaccharide (LPS)-stimulated macrophages treated with KT109.[4] Treatment of mice with KT109 produced antinociceptive activity in the lipopolysaccharide (LPS) inflammatory pain model as well as in nerve injury and paclitaxel neuropathic pain models.[11] These results are consistent with established roles for PGE2 and TNF-α inflammatory signaling in sensitization of peripheral sensory neurons in chronic pain[17,18] and the effectiveness of KT109 to block these pathways *in vivo*.[11] Results from the mouse pain models also showed that local injection of KT109 in the LPS-treated inflamed paw reversed allodynic pain responses, presumably through disruption of DAGLβ function in macrophages that accumulate at inflammatory sites.[17,18]

Here, we set out to test whether we could use liposomes to localize delivery of DAGLβ inhibitors to macrophages *in vivo*. We hypothesized that our approach would not only support macrophages as the site of action but also establish a new strategy for development of targeted anti-inflammatory agents. We developed an encapsulation strategy compatible with the hydrophobic nature of KT109 to produce homogeneous liposomal formulations suitable for *in vivo* testing. We used DAGLβ-tailored activity-based probes and chemical proteomic methods to evaluate potency and selectivity of liposomal KT109 across cells and tissues from treated mice. Finally, we tested whether enhanced delivery of liposomal KT109 to macrophages *in vivo* was sufficient to reverse nociceptive behavior in the mouse LPS inflammatory pain model.

EXPERIMENTAL SECTION

Laboratory Animals. Subjects consisted of male C57BL/6J mice obtained from either Jackson Laboratories (Bar Harbor, Maine) or breeding pairs in the Virginia Commonwealth University vivarium for use in LPS pain studies. For selectivity studies, C57BL/6J mice were obtained from breeding pairs in the University of Virginia vivarium. Animal experiments were conducted in accordance with the guidelines of the Institutional Animal Care and Use Committee of each respective institution.

Materials. KT109, HT-01, and fluorophosphonate-rhodamine (FP-Rh) were synthesized and purity confirmed by ^{1}H-NMR and HPLC analysis as previously described.[4,15,19] Isoflurane (Isothesia, Henry Schein) was purchased from the Center for Comparative Medicine at University of Virginia. Brewer thioglycollate medium was purchased from Fluka Analytical. The following lipids were purchased from Avanti polar lipids as 25 mg/mL stock solutions in chloroform: 1,2-

DOI: 10.1021/acs.molpharmaceut.7b00657
Mol. Pharmaceutics XXXX, XXX, XXX−XXX

dioleoyl-*sn*-glycero-3-phosphoethanolamine (DOPE); 1,2-distearoyl-*sn*-glycero-3-phosphocholine (DSPC); and 1,2-dioleoyl-*sn*-glycero-3-phosphoethanolamine-*N*-[methoxy(polyethylene glycol)-2000] (ammonium salt) (PEG2000 PE). The liposome extrusion kit and polycarbonate membranes were also purchased through Avanti polar lipids. Sepharose beads (Sepharose CL-4B, 20% ethanol) were purchased from GE Health Care, Inc.

Preparation and Characterization of Liposomal KT109. Liposomal KT109 and matching "ghost" liposomes (containing the same lipid components but no compound) were prepared as described in detail in the methods section of the Supporting Information. Ghost liposomes were used as controls for *in vitro* and *in vivo* experiments. All liposomal KT109 stocks were made up as 1 mL sample sizes, limited by the 1 mL total volume of the extrusion syringes. However, multiple sets of liposomes were often made simultaneously to deliver larger quantities of liposomes for experimental use. Liposomal KT109 size and homogeneity were characterized via dynamic light scattering (DLS, Malvern Zetasizer, Nano Series) and nanoparticle tracking analysis (NTA, Malvern NanoSight LM10). KT109 concentrations in liposomes were determined by LC−MS as described below. Liposomes were kept refrigerated and used within a month.

Quantification of KT109 in Liposomal KT109 Stocks by LC−MS. LC−MS was performed on an I-class Acquity coupled to a TQ-S mass spectrometer (Waters Corporation, Milford, MA). Samples were analyzed on a 2.1 mm ID × 5 cm C8 Kinetex column (Phenomenex) with the column oven set to 50 °C. Mobile phases consisted of water with 0.1% formic acid (A) and methanol with 0.1% formic acid (B). A gradient of 50% B to 99% B over 1 min was held for 0.5 min before re-equilibration at 0.5 mL/min. KT109 was detected by multiple reaction monitoring (MRM) analysis using the 423.3 > 202.1 transition with a collision energy of 10 using argon as the collision gas. Concentrations of KT109 in liposomal KT109 stocks were estimated to be ∼20 μg/mL by LC−MS (Figure S1).

***In Vivo* Studies Using Liposomal KT109.** C57BL/6J mice were injected with thioglycollate solution (4% w/v) in the peritoneal cavity 4 days prior to compound treatment in order to recruit sufficient macrophages for analyses. Mice were treated with ghost or liposomal KT109 (2.5 or 5 μg; intraperitoneal, i.p.; 4 h), anesthetized with isoflurane, sacrificed, and thioglycollate-elicited macrophages harvested as previously described.[4] For selectivity profiling, other tissues were harvested at the same time as macrophages. Macrophages and tissues were either used immediately or flash frozen in liquid nitrogen and stored at −80 °C until use.

Preparation of Tissue Proteomes. Tissues were washed twice with ice cold lysis buffer (0.25 M sucrose, 20 mM HEPES, and 2 mM DTT in ddH_2O). Tissues were processed using dounce homogenization and placed in ice for 15 min. Tissue homogenates were centrifuged at 800 × *g* for 5 min at 4 °C. The resulting supernatant was isolated to remove debris. Supernatants were centrifuged at 100,000 × *g* for 45 min at 4 °C. The supernatant was removed and remaining pellet resolubilized in assay buffer (20 mM HEPES in ddH_2O) by passing through a 26-gauge syringe multiple times, and referred to as soluble and membrane fractions, respectively. Protein concentrations were determined using a Bio-Rad DC protein assay.

Gel-Based Competitive Activity Based Protein Profiling (ABPP). Proteomes (1 mg/mL) were treated with either HT-01 or FP-Rh at 1 μM final concentration for 30 min at 37 °C. The reaction was quenched using SDS-PAGE loading buffer. After separation by SDS-PAGE (10% acrylamide), samples were visualized by in-gel fluorescence scanning using a Chemidoc MP imaging system.

Evaluation of Liposomal KT109 in LPS Model of Inflammatory Pain. Mice were given an injection of 2.5 μg of LPS from *Escherichia coli* (026:B6, Sigma), in 20 μL of physiological sterile saline (Hospira Inc., Lake Forest, IL, USA) into the plantar surface of the right hind paw. As previously reported, this dose of LPS elicits mechanical allodynia without producing measurable increases in paw thickness.[20] Mice were returned to their home cages after the LPS injection. Twenty-two hours following LPS administration, each mouse was given an intraperitoneal (i.p.) injection of ghost liposome or liposomal KT109 (8, 4, or 1 μg) and tested for mechanical allodynia at 24 h.

Behavioral Assessment of Mechanical Allodynia. Baseline responses to light mechanical touch were assessed using von Frey filaments following habituation to the testing environment, as described elsewhere.[21] In brief, mice were acclimated to the testing conditions in which they were given a daily 30 min habituation session for 4 days. They were placed under an inverted wire mesh basket, which allowed unrestricted air flow, that was on top of a wire mesh screen, with spaces 0.5 mm apart. During acclimation and testing, each mouse was unrestrained and singly housed. The von Frey test utilizes a series of calibrated monofilaments, (2.83−4.31 log stimulus intensity; North Coast Medical, Morgan Hills, CA, USA) applied randomly to the left and right plantar surfaces of the hind paw for 3 s. Lifting, licking, or shaking the paw was considered a response.

Statistical Analysis. Enzyme activity remaining was determined by comparing integrated band intensities of inhibitor with vehicle-treated samples for gel-based ABPP assays. Linear regression analysis was used to generate KT109 standard curves from LC−MS studies. In the LPS inflammatory pain study, Holm−Sidak's multiple comparisons test was used for post hoc analysis following a significant one-way ANOVA. The antinociceptive ED_{50} value 95% confidence limit of liposomal KT109 was calculated using least-squares linear regression analysis. The potency ratio with 95% confidence limit of KT109 between its formulation in liposomes (present study) and free compound in a standard vehicle (previous study[11]) was calculated using linear regression.[22] Data are shown as mean ± SEM. For analysis of DAGLβ inhibition in paw, significance was determined by unpaired Student's *t* test. All statistical analyses were performed using GraphPad Prism or Excel.

RESULTS

Encapsulation of KT109 in Liposomes. As KT109 is insoluble in aqueous media, typical passive loading mechanisms for liposomal encapsulation were ineffective. We therefore explored whether KT109 could be trapped within the lipid bilayer during the dry-down step of the liposome formulation process. In brief, KT109 was dissolved in chloroform along with a cocktail of natural and unnatural phospholipids. Next, the KT109/lipid mixture was dried down under a nitrogen stream. Addition of aqueous buffer (PBS) followed by shaking and vortexing produced liposomal KT109 (see Methods section in

DOI: 10.1021/acs.molpharmaceut.7b00657
Mol. Pharmaceutics XXXX, XXX, XXX−XXX

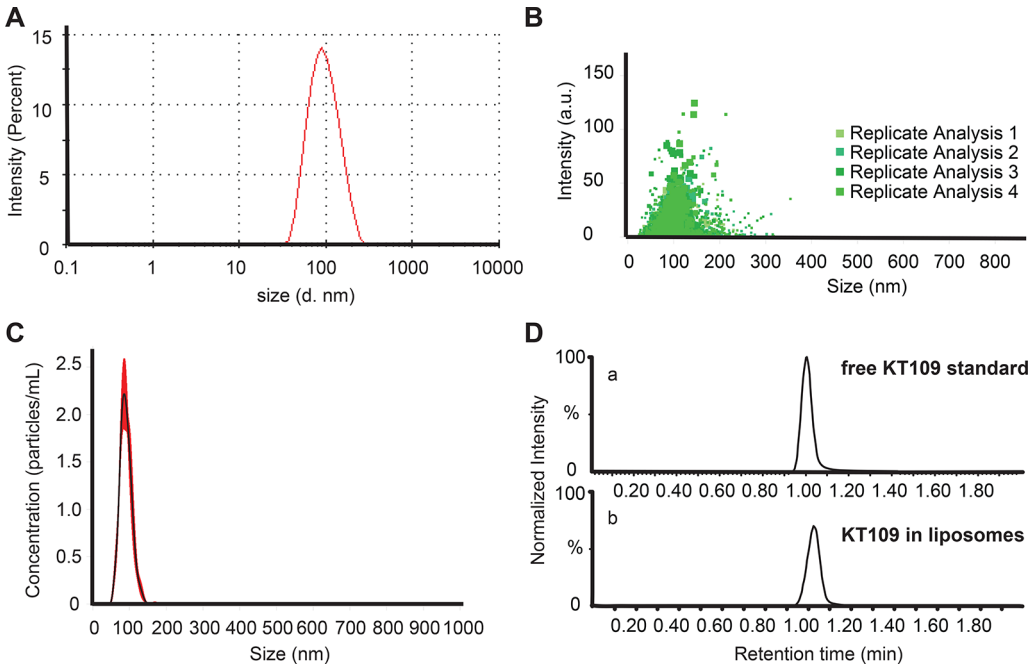

Figure 2. Characterization of liposomal KT109 by DLS, NTA, and LC−MS. (A) Graph showing the average size distribution by intensity of liposomal KT109 as determined by dynamic light scattering (DLS). Liposomal KT109 was diluted 1:100 for this analysis. The peak average is 101 ± 2 nm, which corresponds to a *Z*-average of 89 ± 0.3 nm. (B) Liposomal KT109 size and homogeneity as characterized by nanoparticle tracking analysis (NTA). Representative scatter graph of four replicate analyses of liposomal KT109 intensity (absorbance unit, a.u.) as a function of size (nm). (C) Finite track length adjustment (FTLA) analysis of scatter graphs is used to calculate average particle concentration (9 ± 0.5 × 10^8 particles/mL) and mean particle size (91 ± 2 nm). (D) Representative extracted ion chromatogram from MRM analysis by LC−MS of free KT109 standard compared with KT109 in liposomes. The equivalent retention times confirm the identity of KT109 encapsulated in liposomes. MRM analysis was performed using a 423 to 202 transition for KT109.

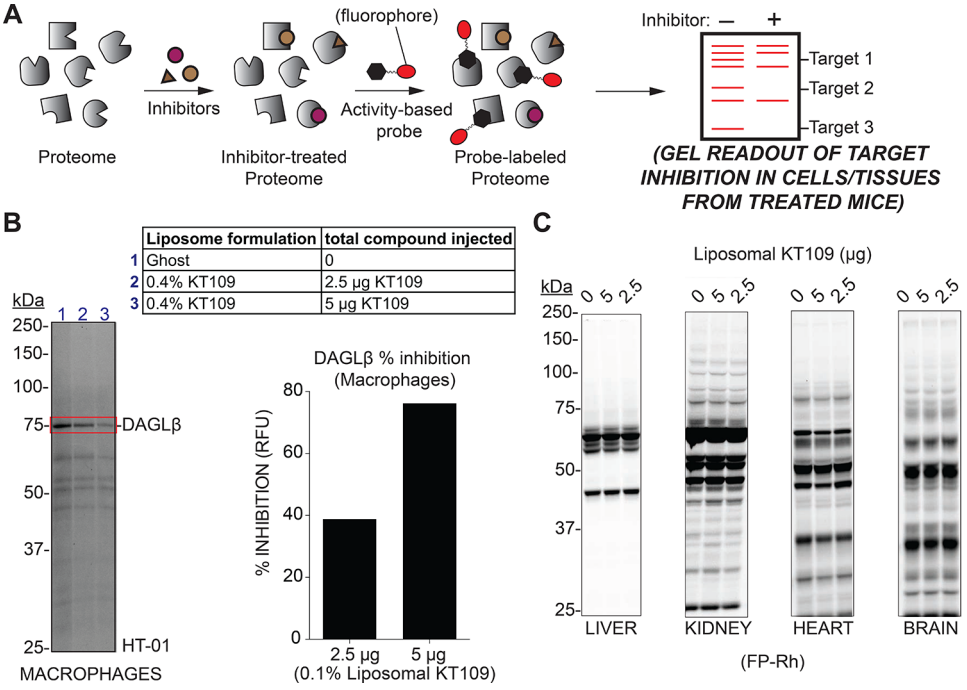

Figure 3. Chemical proteomic evaluation of liposomal KT109 potency and selectivity *in vivo*. (A) General scheme of competitive gel-based activity based protein profiling (ABPP). Proteomes were pretreated with inhibitors (30 min at 37 °C) followed by labeling with activity based probe (HT-01 or FP-Rh, 1 μM, 30 min at 37 °C). Probe-labeled proteomes were separated by SDS-PAGE and analyzed by in-gel fluorescence scanning. (B) Thioglycollate-elicited macrophages were isolated after 4 h treatment with ghost liposomes or liposomal KT109 at the indicated doses. Cells were lysed and membrane proteomes subjected to gel-based ABPP analysis using HT-01. The degree of inactivation (% inhibition) was quantified using integrated band intensities from fluorescence gel analyses. (C) Activity and selectivity of liposomal KT109 against serine hydrolases detected in tissues from treated mice using gel-based ABPP with FP-Rh. Treatment with liposomal KT109 resulted in negligible activity across measured tissues.

DOI: 10.1021/acs.molpharmaceut.7b00657
Mol. Pharmaceutics XXXX, XXX, XXX−XXX

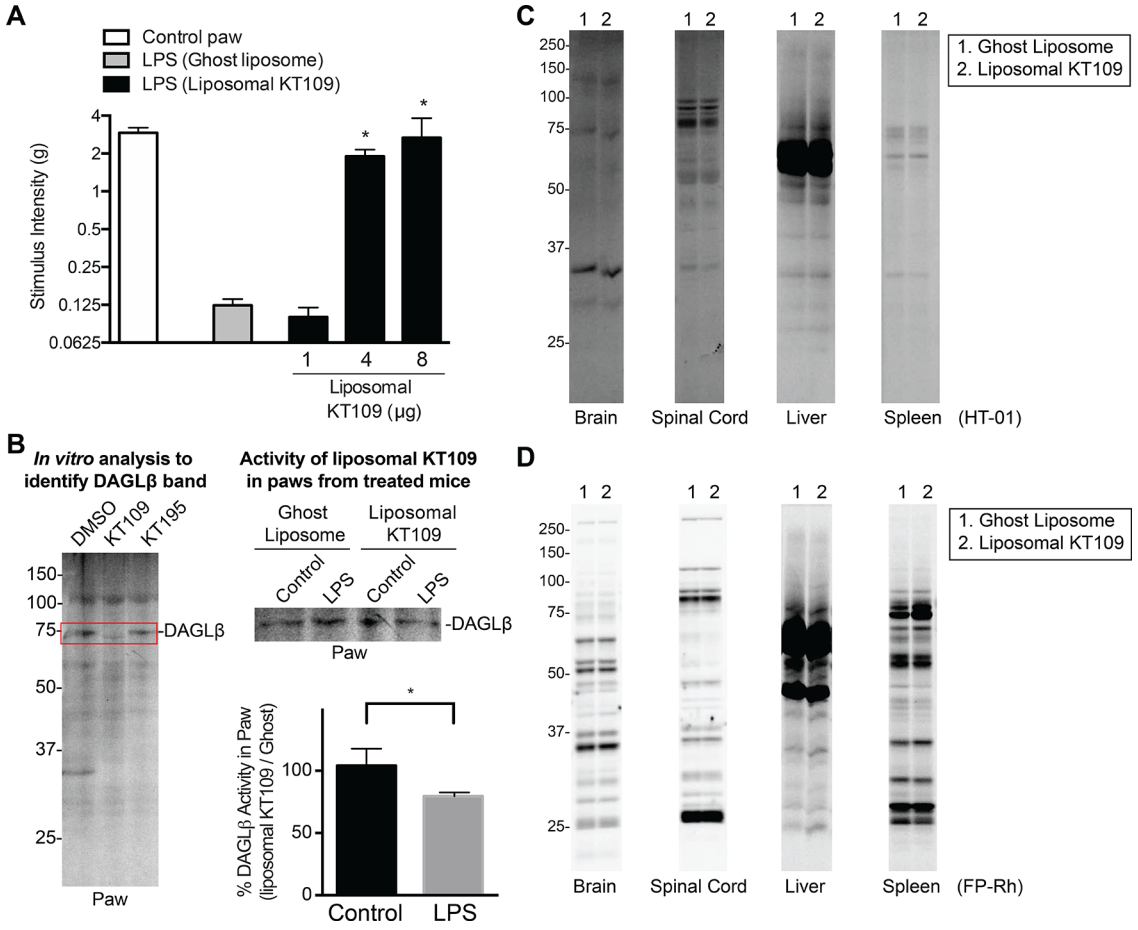

Figure 4. Efficacy and selectivity of liposomal KT109 in the LPS inflammatory pain model. (A) Intraperitoneal (i.p.) administration of liposomal KT109 reverses LPS-induced allodynia in C57BL/6J mice. *P < 0.05 vs LPS + ghost liposome-treated paw. Data reflect mean ± SEM, n = 13 (control paw), 10 (LPS + ghost liposome), 6 (LPS + liposomal KT109 (1 μg)), 6 (LPS + liposomal KT109 (4 μg)), and 3 (LPS + liposomal KT109 (8 μg)). (B) Native DAGLβ activity in LPS-treated and contralateral hind paws (control) from representative mice was measured by gel-based ABPP using HT-01. The identity of the DAGLβ band detected in paws was confirmed by *in vitro* treatment of paw proteomes using free KT109 (DAGLβ specific inhibitor) compared with the DAGLβ-inactive control inhibitor KT195[4] (left panel). Native DAGLβ activity was quantified in paws of mice treated with ghost liposome or liposomal KT109 under basal and inflammatory states (LPS-injected paw). Intraperitoneal administration of liposomal KT109 (4 μg) resulted in ∼20% inhibition of total DAGLβ activity in the LPS-treated paw (estimated by ratio of fluorescent signals of DAGLβ band from paws of liposomal KT109- compared with ghost liposome-treated mice). Liposomal KT109 (4 μg) did not inhibit DAGLβ activity in contralateral paw (no LPS treatment). *P < 0.05 for DAGLβ activity remaining in LPS-injected versus contralateral paws. Liposomal KT109 (4 μg, i.p.) showed negligible activity against serine hydrolases in brain, spinal cord, liver, and spleen of treated mice (under inflammatory states) as measured by gel-based ABPP using HT-01 (C) and FP-Rh (D).

the Supporting Information for more details). Although this method provided us a route for liposomal KT109 formulation, the method proved to be very inefficient with a large portion of compound remaining suspended within the PBS solution rather than entrapped within the lipid bilayer during spontaneous liposome formation upon rehydration. To counter this issue, we used a higher starting concentration of KT109 (5 mg/mL) to overcome limitations resulting from encapsulation inefficiency. More than 99% of the nonencapsulated KT109 is separated from liposomal KT109 during the liposome extrusion step, remaining trapped on one side of the polycarbonate membrane. The remaining free drug is separated from the liposome portion during size-exclusion chromatography to yield pure liposomal KT109.

Characterization of Liposomal KT109. To determine the size and homogeneity of liposomal KT109, we measured these parameters by both dynamic light scattering (DLS) and nanoparticle tracking analysis (NTA). As shown in Figure 2A, the DLS profile revealed a single peak that centers around 101 ± 2 nm in diameter, which corresponds to a Z-average value of 89 ± 0.3 nm in diameter. Like DLS, NTA measures the Brownian motion of particles in a suspension and their speed related to the Stokes−Einstein equation. However, unlike DLS, which can only measure time-dependent fluctuations in scattering intensity, NTA can measure individual particle motion by video. NTA, therefore, is able to provide a more quantitative analysis as well as enhanced size resolution. For NTA, a laser beam is passed through the liposomal suspension. As the liposomes scatter light, they may be visualized by microscope. A representative distribution plot of liposome intensity as a function of size as measured by NTA is shown in Figure 2B. As shown in Figure 2C, we used NTA finite track length adjustment (FTLA) analysis to calculate the average particle concentration ($9 \pm 0.5 \times 10^8$ particles/mL) and a mean particle size (91 ± 2 nm) for a typical liposomal KT109 sample. In summary, characterization of liposomal KT109 using complementary DLS and NTA techniques confirm that stable,

DOI: 10.1021/acs.molpharmaceut.7b00657
Mol. Pharmaceutics XXXX, XXX, XXX−XXX

homogeneous liposomes of desired diameter are routinely and reproducibly fabricated.

To determine the concentration of KT109 encapsulated in liposome, we developed a targeted multiple-reaction monitoring (MRM) LC−MS method to quantify KT109 concentrations in liposome samples (423 to 202 MRM transition, Figure 2D). We first generated a standard curve of free KT109 and showed high correlation between KT109 concentrations and MRM signal intensities from 0.0025 to 0.25 μg/mL (R^2 = 0.99, Figure S1). Using our standard curve, we were able to estimate the concentration of encapsulated KT109 as ∼20 μg/mL (Figure S1). We calculated encapsulation efficiency based on the ratio of total encapsulated (20 μg) versus starting (5 mg) KT109 amounts, which results in an estimated efficiency of ∼0.4%. Future studies will be required to improve the formulation process and increase the amount of KT109 that is effectively incorporated into liposomes.

Chemical Proteomic Analysis of Liposomal KT109. Using our first generation liposomal KT109 formulation, we asked how liposome delivery would impact KT109 potency and selectivity *in vivo*. For these analyses, we evaluated native DAGLβ and other serine hydrolase (SH) activities by gel-based competitive ABPP using DAGL-tailored (HT-01[4]) and broad spectrum (FP-Rh[23]) SH probes (Figure 3A). ABPP analysis provides a molecular snapshot of liposomal KT109 bioavailability and selectivity *in vivo* because covalent enzyme inactivation by KT109 during treatment is not affected by tissue lysis and processing. Mice were treated with ghost liposome or liposomal KT109 (2.5 or 5 μg) for 4 h, animals sacrificed, and tissues processed and analyzed by gel-based ABPP assay (Figure 3A). Remarkably, we observed dose-dependent inhibition of DAGLβ in peritoneal macrophages despite these low amounts of administered KT109 with ∼80% inhibition observed at the 5 μg dose (Figure 3B). Compared with administration of free KT109 (5 mg kg^{-1} dose[4]), liposomal delivery reduced the amount of total KT109 required for comparable DAGLβ inactivation in peritoneal macrophages by >20-fold (∼120 vs 5 μg of KT109 in free- compared with liposomal-delivery, respectively).

We observed excellent selectivity for liposomal KT109 across other tissues profiled (Figures 3C and S2−S5). We measured tissues where DAGLβ is known to be active (liver,[2,4] brain[9]) as well as tissues that are potential liabilities for compound toxicity (kidney, heart). In all tissues profiled, we observed negligible cross-reactivity with the exception of a minor off-target activity against a ∼35 kDa serine hydrolase in kidney (Figure S2) and heart (Figure S3) proteomes that is likely ABHD6 based on molecular weight and reactivity with HT-01 probe.[24] ABHD6 is a known off-target for several mechanism-based inhibitors including triazole ureas like KT109.[4] Gel-based ABPP analysis of brain and liver proteomes from liposomal KT109-treated mice did not reveal any overt off-target activity (Figures 3C and S4−S5). In summary, we discovered that liposomal delivery of KT109 dramatically enhances potency against DAGLβ in macrophages while minimizing cross-reactivity in other tissues where DAGLβ is active.

Liposomal KT109 Exhibits High Potency in Reversing LPS-Induced Mechanical Allodynia. Next, we examined whether liposomal KT109 would reverse LPS-induced mechanical allodynia with increased potency compared with free compound from our recent study.[11] As shown in Figure 4A, KT109 significantly reversed LPS-induced allodynia [$F(4,33) = 32$, $p < 0.0001$]. Post hoc testing revealed that treatment with 4 and 8 μg of liposomal KT109 significantly attenuated LPS-induced allodynia compared with mice receiving LPS and ghost liposomes. At 8 μg of KT109, we observed full reversal of LPS-induced allodynia (Figure 4A). Using these data, the calculated ED_{50} value for liposomal KT109 was 11 μg/kg (9−13 μg/kg; 95% confidence limits), which represents a >100-fold enhancement in potency compared with treatments using free KT109.[11]

We also confirmed that liposomal KT109 was active in the LPS-injected paw by directly measuring native DAGLβ activity at this site by gel-based ABPP using HT-01 (Figure 4B). First, we confirmed that the ∼70 kDa band detected in paw proteomes represented endogenous DAGLβ by demonstrating that pretreatment with KT109 (DAGLβ inhibitor) but not KT195 (DAGLβ-inactive control inhibitor) *in vitro* blocked HT-01 probe labeling (left panel, Figure 4B). Next, we measured DAGLβ activity in contralateral (control) and LPS-injected paws of mice treated with ghost liposome or liposomal KT109. We observed a modest but significant decrease in endogenous DAGLβ activity (∼20% inhibition, $P = 0.037$) in the LPS-injected but not contralateral control paw (right panels, Figure 4B). Future studies are needed to determine whether increased accumulation of macrophages at inflammatory sites is a likely mechanism explaining why liposomal KT109 blocks DAGLβ activity only in the LPS-injected paw. In contrast to activity in the LPS-injected paw, we observed no apparent inhibition of other SHs in central (brain and spinal cord) and peripheral (liver and spleen) tissues from liposomal KT109-treated mice as measured by gel-based ABPP (Figure 4C,D). Collectively, our results help support that liposomal delivery of KT109 dramatically enhances *in vivo* efficacy and selectivity and that the LPS-injected paw is the likely site of action for reversal of LPS-induced allodynia.

DISCUSSION

DAGLβ expression and activity is enriched in macrophages,[4] providing an opportunity to exploit the phagocytic capacity of these immune cells[25] for targeted delivery of inhibitors. We explored liposomal delivery of KT109 with the goal of lowering the total amount of compound required for DAGLβ inactivation in macrophages *in vivo*. The effective increase in potency using liposomal KT109 would allow for more localized blockade of PGE2 and TNF-α signaling at inflammatory sites where macrophages are known to accumulate.[17,18]

We discovered that systemic delivery of ∼5 μg of KT109 in liposomes was sufficient to achieve ∼80% inactivation of DAGLβ in macrophages. Enhanced delivery of liposomal KT109 to macrophages *in vivo* was sufficient to reverse nociceptive behavior in the mouse LPS inflammatory pain model. The calculated ED_{50} value for liposomal KT109 was 11 μg/kg (9−13 μg/kg; 95% confidence limits), which represents a >100-fold enhancement in potency compared with treatments using free KT109.[11] While active in macrophages, the use of liposomal delivery resulted in negligible activity of KT109 in central as well as peripheral tissues under basal (Figures 3C and S2−S5) and inflammatory states (Figure 4C,D). The dramatic increase in potency supports our hypothesis that systemic administration of liposomal KT109 results in accumulation and targeted disruption of DAGLβ activity in macrophage *in vivo*. As a result, we can reduce the total amount of KT109 required for efficacy to minimize cross-reactivity in other tissues and improve overall selectivity *in vivo*.

DOI: 10.1021/acs.molpharmaceut.7b00657
Mol. Pharmaceutics XXXX, XXX, XXX−XXX

We also demonstrated that chemical proteomic methods were critical for evaluating the cells and tissues where liposomal KT109 is active. Importantly, the use of HT-01-based ABPP analysis allowed us to confirm potent inactivation of DAGLβ in macrophages as well as to measure general off-target activity against other detected SHs in central and peripheral tissues. An interesting finding from our chemical proteomics analyses was detection of DAGLβ inhibition by liposomal KT109 only in the LPS-injected paw (Figure 4B). While we cannot fully explain why DAGLβ activity was unaffected in control paws, our current findings support macrophages as the likely site of action for the antinociceptive activity of liposomal KT109. Future studies will focus on isolation of macrophages from paws of treated mice to further clarify the specificity of liposomal KT109 for targeting macrophages versus other cell types at inflammatory sites. We are also cognizant that DAGLβ inactivation at other sites in addition to the paw may contribute to the observed efficacy *in vivo*. Future studies are needed to investigate whether changes in macrophage trafficking and/or phagocytic capacity affects liposomal KT109 access and clearance during inflammation, and whether this could represent a general strategy to target compounds to inflammatory sites. Incorporation of targeting agents, e.g., antibodies against the macrophage-specific marker F4/80,[26] in future studies should further enhance the utility of this approach to target specific macrophage subsets.

While our preliminary studies using liposomal KT109 were successful, we recognize the low encapsulation efficiency of our current formulation process. Currently the encapsulation efficiency of KT109 within the formulated liposomes is ~0.4%. Concentrating liposomes can increase the effective dose administered *in vivo* but does not address the substantial loss of KT109 during formulation. Future studies therefore, in addition to the incorporation of targeting agents, should also address the suboptimal encapsulation efficiencies. Different methods of liposomal loading and/or lipid formulation are presently being considered. Other nanoparticle materials, specifically block copolymers such as PLGA and PLA/PEO formulations,[27,28] are also being considered for potential improvement of KT109 encapsulation.

■ ASSOCIATED CONTENT

Supporting Information

The Supporting Information is available free of charge on the ACS Publications website at DOI: 10.1021/acs.molpharmaceut.7b00657.

Details on liposome preparation and supplementary figures (PDF)

■ AUTHOR INFORMATION

Corresponding Author

*Address: Department of Chemistry and Department of Pharmacology, University of Virginia, McCormick Road, P.O. Box 400319, Charlottesville, Virginia 22904, United States. E-mail: kenhsu@virginia.edu. Phone: 434-297-4864.

ORCID

Ku-Lung Hsu: 0000-0001-5620-3972

Author Contributions

#These authors contributed equally.

Notes

The authors declare no competing financial interest.

■ ACKNOWLEDGMENTS

We thank all members of the Hsu Lab and colleagues at the University of Virginia for helpful discussions and review of the manuscript. This work was supported by the University of Virginia (start-up funds to K.-L.H.), VCU School of Pharmacy (start-up funds to A.H.L.), NanoSTAR (to H.S.), and National Institutes of Health (DA035864 to K.-L.H.; 1F31NS095628 to L.D.S.; T32DA007027, P30DA033934, and R01NS093990 to A.H.L.).

■ ABBREVIATIONS

ABPP, activity based protein profiling; DAGLβ, diacylglycerol lipase-beta; DAGLα, diacylglycerol lipase-alpha; AA, arachidonic acid; COX, cyclooxygenase; DAG, diacylglycerol; GPCR, G-protein-coupled receptor; LPS, lipopolysaccharide; FP-Rh, fluorophosphonate-rhodamine; DOPE, 1,2-dioleoyl-*sn*-glycero-3-phosphoethanolamine; DSPC, 1,2-distearoyl-*sn*-glycero-3-phosphocholine; PEG2000 PE, 1,2-dioleoyl-*sn*-glycero-3-phosphoethanolamine-*N*-[methoxy(polyethylene glycol)-2000]; i.p., intraperitoneal; DLS, dynamic light scattering; NTA, nanoparticle tracking analysis; FTLA, finite track length adjustment; MRM, multiple-reaction monitoring; LC−MS, liquid chromatography−mass spectrometry; NSAIDs, non-steroidal anti-inflammatory drugs; TNF-α, tumor necrosis factor-alpha; PGE2, prostaglandin E2; PLGA, poly(lactide-*co*-glycolide); PLA/PEO, poly(lactic acid)−poly(ethylene oxide)

■ REFERENCES

(1) Bisogno, T.; Howell, F.; Williams, G.; Minassi, A.; Cascio, M. G.; Ligresti, A.; Matias, I.; Schiano-Moriello, A.; Paul, P.; Williams, E. J.; Gangadharan, U.; Hobbs, C.; Di Marzo, V.; Doherty, P. Cloning of the first sn1-DAG lipases points to the spatial and temporal regulation of endocannabinoid signaling in the brain. *J. Cell Biol.* **2003**, *163* (3), 463−8.

(2) Gao, Y.; Vasilyev, D. V.; Goncalves, M. B.; Howell, F. V.; Hobbs, C.; Reisenberg, M.; Shen, R.; Zhang, M. Y.; Strassle, B. W.; Lu, P.; Mark, L.; Piesla, M. J.; Deng, K.; Kouranova, E. V.; Ring, R. H.; Whiteside, G. T.; Bates, B.; Walsh, F. S.; Williams, G.; Pangalos, M. N.; Samad, T. A.; Doherty, P. Loss of Retrograde Endocannabinoid Signaling and Reduced Adult Neurogenesis in Diacylglycerol Lipase Knock-out Mice. *J. Neurosci.* **2010**, *30* (6), 2017−24.

(3) Tanimura, A.; Yamazaki, M.; Hashimotodani, Y.; Uchigashima, M.; Kawata, S.; Abe, M.; Kita, Y.; Hashimoto, K.; Shimizu, T.; Watanabe, M.; Sakimura, K.; Kano, M. The endocannabinoid 2-arachidonoylglycerol produced by diacylglycerol lipase alpha mediates retrograde suppression of synaptic transmission. *Neuron* **2010**, *65* (3), 320−7.

(4) Hsu, K. L.; Tsuboi, K.; Adibekian, A.; Pugh, H.; Masuda, K.; Cravatt, B. F. DAGLbeta inhibition perturbs a lipid network involved in macrophage inflammatory responses. *Nat. Chem. Biol.* **2012**, *8* (12), 999−1007.

(5) Mechoulam, R.; Ben-Shabat, S.; Hanus, L.; Ligumsky, M.; Kaminski, N. E.; Schatz, A. R.; Gopher, A.; Almog, S.; Martin, B. R.; Compton, D. R.; et al. Identification of an endogenous 2-monoglyceride, present in canine gut, that binds to cannabinoid receptors. *Biochem. Pharmacol.* **1995**, *50* (1), 83−90.

(6) Sugiura, T.; Kondo, S.; Sukagawa, A.; Nakane, S.; Shinoda, A.; Itoh, K.; Yamashita, A.; Waku, K. 2-Arachidonoylglycerol: a possible endogenous cannabinoid receptor ligand in brain. *Biochem. Biophys. Res. Commun.* **1995**, *215* (1), 89−97.

(7) Mackie, K. Cannabinoid receptors as therapeutic targets. *Annu. Rev. Pharmacol. Toxicol.* **2006**, *46*, 101−22.

(8) Rouzer, C. A.; Marnett, L. J. Endocannabinoid oxygenation by cyclooxygenases, lipoxygenases, and cytochromes P450: cross-talk between the eicosanoid and endocannabinoid signaling pathways. *Chem. Rev.* **2011**, *111* (10), 5899−921.

DOI: 10.1021/acs.molpharmaceut.7b00657
Mol. Pharmaceutics XXXX, XXX, XXX−XXX

(9) Viader, A.; Ogasawara, D.; Joslyn, C. M.; Sanchez-Alavez, M.; Mori, S.; Nguyen, W.; Conti, B.; Cravatt, B. F. A chemical proteomic atlas of brain serine hydrolases identifies cell type-specific pathways regulating neuroinflammation. *eLife* **2016**, *5*, e12345.
(10) Deng, H.; Kooijman, S.; van den Nieuwendijk, A. M.; Ogasawara, D.; van der Wel, T.; van Dalen, F.; Baggelaar, M. P.; Janssen, F. J.; van den Berg, R. J.; den Dulk, H.; Cravatt, B. F.; Overkleeft, H. S.; Rensen, P. C.; van der Stelt, M. Triazole Ureas Act as Diacylglycerol Lipase Inhibitors and Prevent Fasting-Induced Refeeding. *J. Med. Chem.* **2017**, *60* (1), 428−440.
(11) Wilkerson, J. L.; Ghosh, S.; Bagdas, D.; Mason, B. L.; Crowe, M. S.; Hsu, K. L.; Wise, L. E.; Kinsey, S. G.; Damaj, M. I.; Cravatt, B. F.; Lichtman, A. H. Diacylglycerol lipase beta inhibition reverses nociceptive behaviour in mouse models of inflammatory and neuropathic pain. *Br. J. Pharmacol.* **2016**, *173* (10), 1678−92.
(12) Ogasawara, D.; Deng, H.; Viader, A.; Baggelaar, M. P.; Breman, A.; den Dulk, H.; van den Nieuwendijk, A. M.; Soethoudt, M.; van der Wel, T.; Zhou, J.; Overkleeft, H. S.; Sanchez-Alavez, M.; Mori, S.; Nguyen, W.; Conti, B.; Liu, X.; Chen, Y.; Liu, Q. S.; Cravatt, B. F.; van der Stelt, M. Rapid and profound rewiring of brain lipid signaling networks by acute diacylglycerol lipase inhibition. *Proc. Natl. Acad. Sci. U. S. A.* **2016**, *113* (1), 26−33.
(13) Baggelaar, M. P.; Janssen, F. J.; van Esbroeck, A. C.; den Dulk, H.; Allara, M.; Hoogendoorn, S.; McGuire, R.; Florea, B. I.; Meeuwenoord, N.; van den Elst, H.; van der Marel, G. A.; Brouwer, J.; Di Marzo, V.; Overkleeft, H. S.; van der Stelt, M. Development of an Activity-Based Probe and In Silico Design Reveal Highly Selective Inhibitors for Diacylglycerol Lipase-alpha in Brain. *Angew. Chem.* **2013**, *125*, 12415.
(14) Baggelaar, M. P.; Chameau, P. J.; Kantae, V.; Hummel, J.; Hsu, K. L.; Janssen, F.; van der Wel, T.; Soethoudt, M.; Deng, H.; den Dulk, H.; Allara, M.; Florea, B. I.; Di Marzo, V.; Wadman, W. J.; Kruse, C. G.; Overkleeft, H. S.; Hankemeier, T.; Werkman, T. R.; Cravatt, B. F.; van der Stelt, M. Highly Selective, Reversible Inhibitor Identified by Comparative Chemoproteomics Modulates Diacylglycerol Lipase Activity in Neurons. *J. Am. Chem. Soc.* **2015**, *137* (27), 8851−7.
(15) Hsu, K. L.; Tsuboi, K.; Whitby, L. R.; Speers, A. E.; Pugh, H.; Inloes, J.; Cravatt, B. F. Development and optimization of piperidyl-1,2,3-triazole ureas as selective chemical probes of endocannabinoid biosynthesis. *J. Med. Chem.* **2013**, *56* (21), 8257−69.
(16) Janssen, F. J.; Deng, H.; Baggelaar, M. P.; Allara, M.; van der Wel, T.; den Dulk, H.; Ligresti, A.; van Esbroeck, A. C.; McGuire, R.; Di Marzo, V.; Overkleeft, H. S.; van der Stelt, M. Discovery of glycine sulfonamides as dual inhibitors of sn-1-diacylglycerol lipase alpha and alpha/beta-hydrolase domain 6. *J. Med. Chem.* **2014**, *57* (15), 6610−22.
(17) Costigan, M.; Scholz, J.; Woolf, C. J. Neuropathic pain: a maladaptive response of the nervous system to damage. *Annu. Rev. Neurosci.* **2009**, *32*, 1−32.
(18) Marchand, F.; Perretti, M.; McMahon, S. B. Role of the immune system in chronic pain. *Nat. Rev. Neurosci.* **2005**, *6* (7), 521−32.
(19) Patricelli, M. P.; Giang, D. K.; Stamp, L. M.; Burbaum, J. J. Direct visualization of serine hydrolase activities in complex proteomes using fluorescent active site-directed probes. *Proteomics* **2001**, *1* (9), 1067−71.
(20) Booker, L.; Kinsey, S. G.; Abdullah, R. A.; Blankman, J. L.; Long, J. Z.; Ezzili, C.; Boger, D. L.; Cravatt, B. F.; Lichtman, A. H. The fatty acid amide hydrolase (FAAH) inhibitor PF-3845 acts in the nervous system to reverse LPS-induced tactile allodynia in mice. *Br. J. Pharmacol.* **2012**, *165* (8), 2485−96.
(21) Murphy, P. G.; Ramer, M. S.; Borthwick, L.; Gauldie, J.; Richardson, P. M.; Bisby, M. A. Endogenous interleukin-6 contributes to hypersensitivity to cutaneous stimuli and changes in neuropeptides associated with chronic nerve constriction in mice. *Eur. J. Neurosci* **1999**, *11* (7), 2243−53.
(22) Colquhoun, D. *Lectures on Biostatistics; an Introduction to Statistics with Applications in Biology and Medicine*; Clarendon Press: Oxford, 1971; p xviii.
(23) Jessani, N.; Liu, Y.; Humphrey, M.; Cravatt, B. F. Enzyme activity profiles of the secreted and membrane proteome that depict cancer cell invasiveness. *Proc. Natl. Acad. Sci. U. S. A.* **2002**, *99* (16), 10335−40.
(24) Hsu, K. L.; Tsuboi, K.; Chang, J. W.; Whitby, L. R.; Speers, A. E.; Pugh, H.; Cravatt, B. F. Discovery and optimization of piperidyl-1,2,3-triazole ureas as potent, selective, and in vivo-active inhibitors of alpha/beta-hydrolase domain containing 6 (ABHD6). *J. Med. Chem.* **2013**, *56* (21), 8270−9.
(25) Van Rooijen, N.; Sanders, A. Liposome mediated depletion of macrophages: mechanism of action, preparation of liposomes and applications. *J. Immunol. Methods* **1994**, *174* (1−2), 83−93.
(26) Laroui, H.; Viennois, E.; Xiao, B.; Canup, B. S. B.; Geem, D.; Denning, T. L. Merlin, D. Fab′-bearing siRNA TNFα-loaded nanoparticles targeted to colonic macrophages offer an effective therapy for experimental colitis. *J. Controlled Release* **2014**, *186*, 41−53.
(27) McDaniel, D. K.; Jo, A.; Ringel-Scaia, V. M.; Coutermarsh-Ott, S.; Rothschild, D. E.; Powell, M. D.; Zhang, R.; Long, T. E.; Oestreich, K. J.; Riffle, J. S.; Davis, R. M.; Allen, I. C. TIPS pentacene loaded PEO-PDLLA core-shell nanoparticles have similar cellular uptake dynamics in M1 and M2 macrophages and in corresponding in vivo microenvironments. *Nanomedicine* **2017**, *13* (3), 1255−1266.
(28) Pustulka, K. M.; Wohl, A. R.; Lee, H. S.; Michel, A. R.; Han, J.; Hoye, T. R.; McCormick, A. V.; Panyam, J.; Macosko, C. W. Flash nanoprecipitation: particle structure and stability. *Mol. Pharmaceutics* **2013**, *10* (11), 4367−77.

DOI: 10.1021/acs.molpharmaceut.7b00657
Mol. Pharmaceutics XXXX, XXX, XXX−XXX